SAND95-2328C
CONF-9510161--2

preliminary version, not camera ready

Barrier/Cu Contact Resistivity

J.S. Reid*[1], M.S. Angyal***, D. Lilienfeld**, Paul Martin Smith***, Y. Shacham-Diamand**, and M-A. Nicolet*

* California Institute of Technology, Pasadena, California 91125
** Cornell University, Ithaca, New York 14850
*** Sandia National Laboratories, Albuquerque, New Mexico 87185

Abstract–The specific contact resistivity of Cu with (α+β)-Ta, TiN, α-W, and amorphous-$Ta_{36}Si_{14}N_{50}$ barrier films is measured using a novel four-point-probe approach. Geometrically, the test structures consist of colinear sets of W-plugs to act as current and voltage probes that contact the bottom of a planar Cu/barrier/Cu stack. Underlying Al interconnects link the plugs to the current source and voltmeter. The center-to-center distance of the probes ranges from 3 to 200 μm. Using a relation developed by Vu *et al.*, a contact resistivity of roughly 7×10^{-9} Ω cm^2 is obtained for all tested barrier/Cu combinations. By reflective-mode small-angle X-ray scattering, the similarity in contact resistivity among the barrier films may be related to interfacial impurities absorbed from the deposition process.

Introduction

In measuring the specific contact resistance between two metals, device manufacturers often implement a "Kelvin" structure [1]. In its simplest form, the structure consists of a via electrically connecting two planes of metal. A probe to source or sink the current contacts each plane. Two additional probes are used to measure the voltage, *V*, across the planes. By knowing the resistivity and spatial dimensions of the via material, the contribution of the interfacial resistance of the via with the planar metals may be extracted from the total measured resistance. In cases where the contact resistance is very low, numerous vias may be chained together to increase the summed potentials to measurable levels.

Although Kelvin structures are conceptually simple and do mimic the environment within an integrated circuit, they are often difficult to implement and can suffer from current-crowding effects [2,3]. Fabrication usually requires exposing the sample to air after deposition of each metal. Consequently, *in-situ* surface cleaning is often required to remove native oxides from the metals if very low resistances are desired. In many deposition systems, *in-situ* cleans are not possible.

---

1. Current address:
Intel Corporation, 5200 NE Elam Young Parkway, D1-67, Hillsboro, Oregon 97124-6497

DISCLAIMER

DISCLAIMER

Portions of this document may be illegible in electronic image products. Images are produced from the best available original document.

A four-point probe method developed by Vu *et al.* for planar multilayers offers an attractive alternative to Kelvin structures [4]. Figure 1 demonstrates the geometry of the technique. Current and voltage probes are in contact with planar layers of metal which may be deposited without breaking vacuum. Assuming the probes to be colinear and equidistant, the potential between the inner probes is

$$V = \frac{I\ln 2}{\pi}\rho_o + \frac{I\rho_o\rho_{s1}}{\pi\,\rho_{s2}}\left(K_o\left(\frac{s}{a}\right) - K_o\left(\frac{2s}{a}\right)\right) \qquad (1)$$

where,

$$\rho_o = (1/\rho_{s1} + 1/\rho_{s2})^{-1}$$

and

$$a = \left(\frac{2\rho_c}{\rho_{s1} + \rho_{s2}}\right)^{\frac{1}{2}}.$$

Here, ρ_{s1} and ρ_{s2} are the sheet resistances of Cu layers "1" and "2" (in units of Ω/square), ρ_c is the contact resistivity between the two layers (units of Ω cm^2), s is the probe separation, and I is the current. K_0 is the zeroth order Bessel function of the second kind. The first term in (1) is the potential given by the two Cu layers in parallel without any contact resistance. It has no dependence on the probe separation, s. The second term, which depends on s, is the contribution of the contact resistance to the potential. As s increases, the second term monotonically decreases to zero. Consequently, to measure the lowest possible contact resistances, s should be minimized. In deriving Eqn. (1), the sheet resistivity of the barrier is assumed to be much greater than the copper layers. The term, ρ_c, also includes contributions from the transverse (top-to-bottom) resistance of the barrier (resistivity of barrier × barrier thickness). Additionally, a two-dimensional, thin-layer approximation is made in Eqn. (1). That is to say, the vertical potential gradient is neglected within a given layer. When probing a single homogeneous layer, the approximation is excellent if the probe separation is at least twice the layer thickness [1]. To measure the lowest possible contact resistivities, the Cu sheet resistivities should be made as small as possible and satisfy $\rho_{s1} \approx 2\rho_{s2}$.

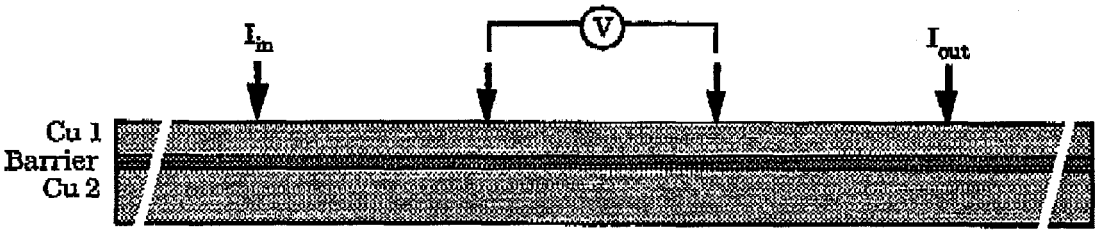

Figure 1. Schematic of the four-point probe technique for extracting barrier/Cu contact resistivity.

Procedure

The approach taken here for fabricating the four-point-probe measurement structures allowed for all photolithographic processing to be completed to prior to Cu contamination of the wafers. Starting material for fabricating the test structures was thermally-oxidized silicon. Sputter-deposited Al (700 nm)/TiN (25 nm) layers were added and then dry-etched through a photoresist mask to define the interconnects and contact pads. Next, 1.7 μm of plasma-enhanced CVD SiO_2 was deposited and planarized with chemical mechanical polishing. The distance between the top of the interconnect and the top surface of the CVD-SiO_2 after the polishing was 500 nm. Next, vias to define the current and voltage probes were dry-etched with a photoresist mask through the oxide to the underlying TiN. Blanket depositions of sputtered, 25-nm TiN liner and 800-nm CVD W followed. Excess TiN/W outside the vias was removed by chemical-mechanical polishing. The colinear sets of W probes had center-to-center spacings of s = 3, 4, 5, 6, 8, 10, 12, 15, 20, 40, and 200 μm. The via widths were 0.4 μm for s = 3-15 μm; 1 μm for s = 20, 40 μm; and 4 μm for s = 200 μm. Openings through the oxide to allow mechanical probing of the contact pads was accomplished by a photoresist mask and BOE etch. Lastly, a 5-μm-thick photoresist layer was applied to allow lift-off of the Cu/barrier/Cu stack, providing electrical isolation between the contact pads and the stack. The lateral dimensions of the exposed region for deposition was at least 20 times the probe spacing to ensure accuracy of Eqn. (1), which assumes an infinite lateral geometry.

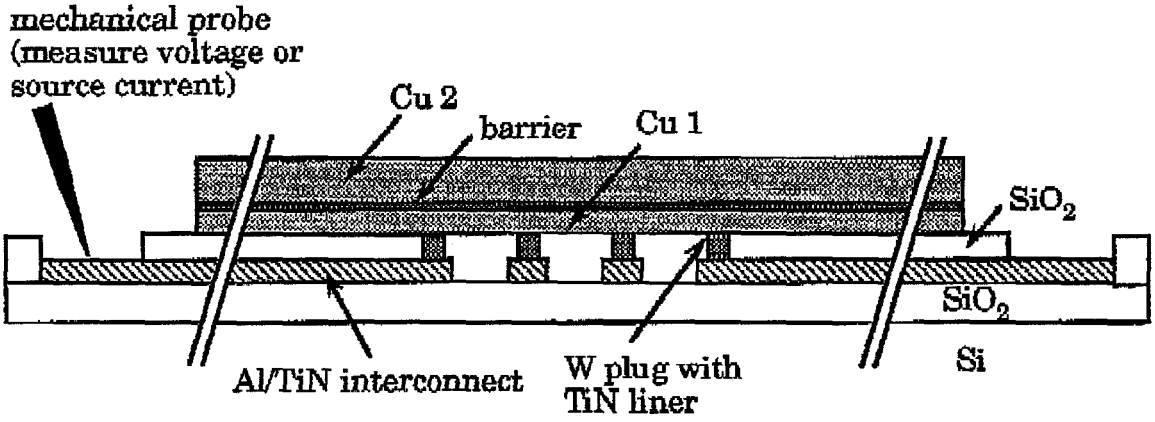

Figure 2. Simplified schematic of final four-point probe test structure to measure barrier/Cu contact resistance. The actual structure had 7 or 11 colinear W plugs serving as current or voltage probes to the Cu/barrier/Cu stack.

Deposition of the trilayer stacks of Cu (420 nm)/barrier (30 nm)/Cu (900 nm) onto the test structures was accomplished in an rf-sputtering system equipped with 7.5-cm-diameter cathodes and fixed magnetrons. The barriers studied were (α+β)-Ta, TiN, α-W, and amorphous-$Ta_{36}Si_{14}N_{50}$. By means of a cryopump and cryogenic

baffle, the base pressure of the system was 2×10^{-7} Torr. With the cryopump throttled for deposition, the base pressure rose to approximately 9×10^{-7} Torr. Just prior to loading into the sputtering system, the test structures were etched for 10 s in 1:30 HF:H_2O and blown dry with N_2. Deposition of Cu was performed in 450 W, 5-mTorr Ar discharges with -50 V of dc substrate bias. (α+β)-Ta and α-W barrier films were deposited in 400 W, 7 mTorr Ar discharges with -50 V substrate bias. The TiN barrier was reactively sputtered in a 450 W, 7-mTorr, Ar/N_2 discharge and -60 V substrate bias. Amorphous $Ta_{36}Si_{14}N_{50}$ barrier films were reactively sputtered in a 10-mTorr Ar/N_2 discharge from a Ta_5Si_3 target with the stage allowed to float electrically. All depositions were performed with the samples residing the perimeter of a large circular stage. During deposition, the stage rotated to cycle the samples underneath the target every ~20 s in a "planetary" mode of operation. Vacuum was maintained between deposition of the individual layers of a given stack. Impurity levels in the Cu, Ta, W, and TiN films were less than or equal to 1 at.% Ar and 1 at.% O, as measured ^{4}He backscattering of the individual films deposited on graphite substrates. The $Ta_{36}Si_{14}N_{50}$ films, however, contained about 2 at.% of both Ar and O. X-ray diffraction of the individual stacks revealed the presence of Cu, (α+β)-Ta, TiN, α-W, amorphous-$Ta_{36}Si_{14}N_{50}$, but no other phases. Following deposition, the trilayer stacks were patterned by lift-off in acetone and annealed for 30 min at 450°C in $<10^{-6}$ Torr vacuum. Figure 2 shows the final geometry of the structures. Mechanical probes contacted pads on the perimeter of the structures to supply current and measure the voltage. The current supply was a Kiethley Model 220 Programmable Current Source set at 10 mA. The voltage was measured with a Kiethley Model 181 Nanovoltmeter.

To extract the contact resistances from a trilayer stack, measurements were taken for each set of probe spacings. The data were then fit with Eqn. (1) using standard least-squares methods. Several structures containing the same probe separation were measured to obtain an estimate of the statistical deviations. Two fit parameters were chosen: the specific contact resistivity, ρ_c, and the copper resistivity, ρ_{Cu}. The copper resistivity was included in Eqn. (1) by substituting ρ_{Cu}/t_i for ρ_{si}, where t_i is the thickness of copper layer i.

Results

Figure 3 shows the measured V/I data and least-squares fits. Because of problems with via conduction or defects in the dielectric, some tested probe combinations yielded unreasonably high or low voltages, or unstable measurements. Such measurements were not included in the analysis. The points in Figure 3 represent the averaged data over several test structures. For probe spacings between s = 15 and 200 μm, the measured data is relatively flat for all of the systems. In this wide-probe regime, the measured potential is purely from the parallel sheet resistances of the copper layers. However, as the probe separation is decreased from 12 to 3 μm, V/I

increases through contact resistance contributions. Deviations in the measurements became more pronounced as the probe spacing decreased, which may be a consequence in nonuniformities in bonding along the barrier/Cu interfaces. Curve fitting yields contact resistivities typically in the mid-10^{-9} Ω cm^2 range with the copper resistivity between 1.8×10^{-6} and 2.1×10^{-6} Ω cm. The actual copper resistivity, measured with a standard four-point-probe on a blanket copper film is 2.0 $\mu\Omega$ cm. Table 1 summarizes the results. The ohmic losses from transversing a barrier's thickness are much less than the measured contact resistivity, thus the ohmic losses are not contributing significantly to the extracted contact resistivity. Considering experimental uncertainty, the relative differences of the extracted values between the various barriers are probably not meaningful.

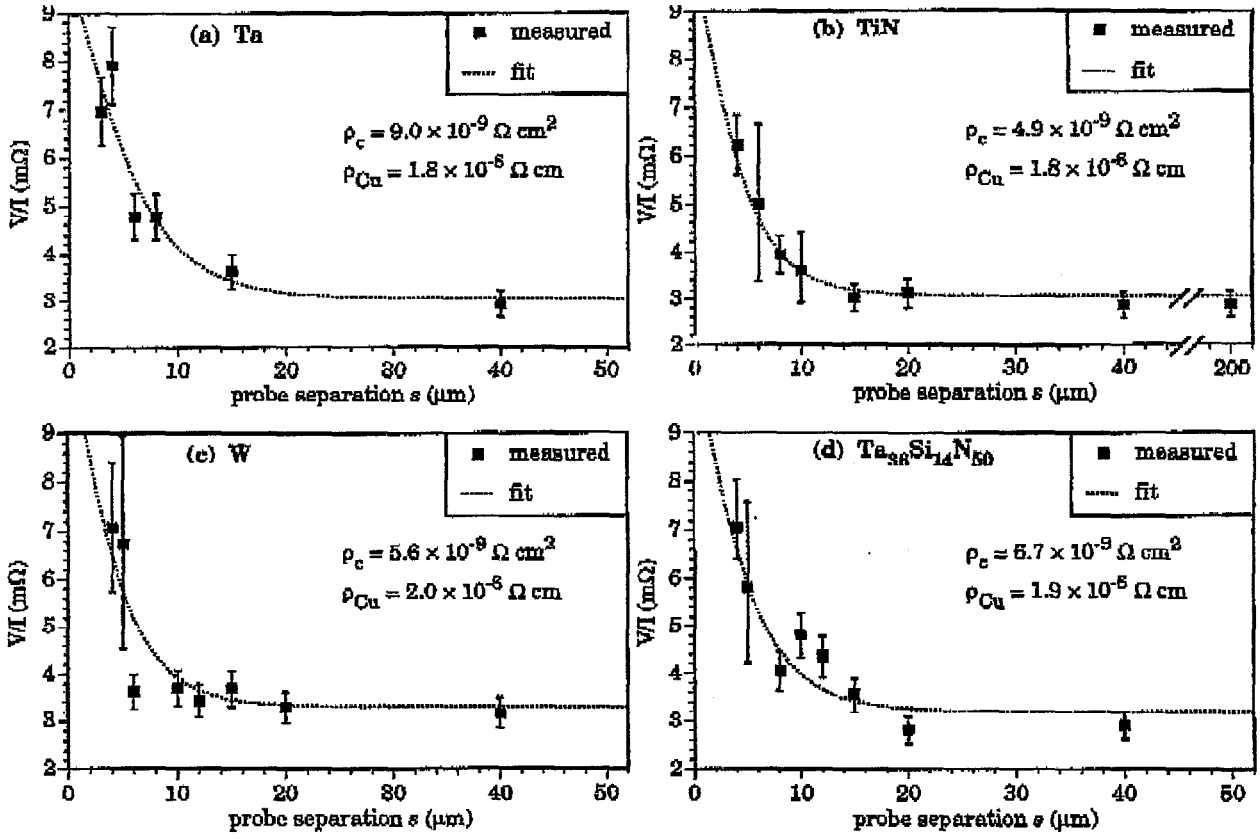

Figure 8. Measured V/I values vs. probe separation, s, along with fits of Eqn. (1) for various diffusion barriers: (a) (α+β)-Ta, (b) TiN, (c) α-W, and (d) amorphous-$Ta_{36}Si_{14}N_{50}$. Error bars were taken as the extremes of the measured values for a given set of probe spacings on separate test structures or ±10% of the average, whichever was larger.

The similarities in the fitted data for the various systems may be a consequence of interfacial impurities absorbed from the deposition process. From residual-gas-analyzer measurements, the partial pressure of H_2O with the pump throttled for deposition is around 2×10^{-7} Torr. Consequently, a couple monolayers of

water vapor bombard the samples every 10 seconds. Given that the samples reside in this vacuum for 5 to 25 min to allow for presputtering between depositions of each layer, there is ample time to grow a thin surface oxide. The effect is easily observed through reflection-mode ("θ-2θ") small-angle X-ray scattering. As an example, Figure 4 shows a spectrum taken from a 400-nm-thick $Ta_{36}Si_{14}N_{50}$ film deposited in a planetary mode. During deposition, the sample was swept under a shutter opening beneath the sputter target every 20 seconds. With every sweep, approximately 3 nm of material was deposited. The small-angle X-ray scan clearly shows periodicities associated with the cycling of substrates beneath the target. Rough simulations of the X-ray spectrum indicate that the oxide thickness grown between passes is a few Angstroms.

Table 1: Summary of curve fitting of the contact resistivity data. The two fit parameters were the copper resistivity, ρ_{Cu}, and the effective specific contact resistivity, ρ_c. For comparison, the calculated contributions to contact resistivity measurement from transverse ohmic losses across the barrier, $(\rho_c)_{transverse}$ (= resistivity of barrier × barrier thickness), is also given. By fitting the extremes of the error bars for $s < 15$ μm and fixing the copper resistivity at 2.0×10^{-6} Ω cm, uncertainty the contact resistivity for all the systems is roughly $\pm 3 \times 10^{-9}$ Ω cm^2.

barrier	ρ_{Cu} (10^{-6} Ω cm)	ρ_c (10^{-9} Ω cm^2)	$(\rho_c)_{transverse}$ (10^{-9} Ω cm^2)
(α+β)-Ta	1.8	9.0	~0.10
TiN	1.8	4.9	~0.20
α-W	2.0	5.6	~0.03
amorphous-$Ta_{36}Si_{14}N_{50}$	1.9	6.9	~2

Conclusion

By using the microscopic four-point-probe technique, the barrier/Cu contact resistivity for the barriers, (α+β)-Ta, TiN, α-W, and amorphous-$Ta_{36}Si_{14}N_{50}$, was measured to be approximately 7×10^{-9} Ω cm^2. The similarities in contact resistivity for the various barriers with Cu may be partially attributable to inadequate vacuum, as demonstrated by small-angle X-ray reflectivity measurements. A key advantage to using the four-point-probe method is the ability to produce the film interfaces without breaking vacuum between layers. Another advantage to using an "upside-down" probing scheme with a lift-off process is the reduced risk of Cu contamination in many clean-room environments. Because the blanket Cu deposition and subsequent lift-off are the final steps of the process, other processing tools such as lithography steppers, ion etchers, or CVD dielectric deposition systems are never exposed to Cu.

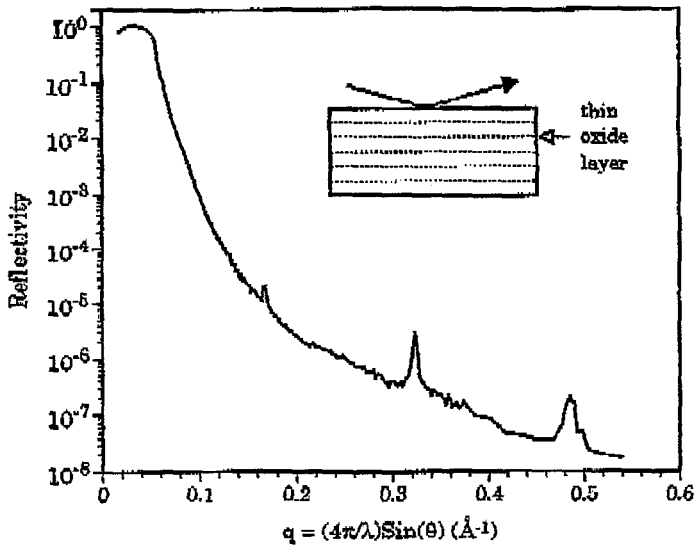

Figure 4. Small-angle X-ray reflectivity pattern of a 400-nm $Ta_{36}Si_{14}N_{50}$ film deposited in a planetary mode.

Acknowledgments

The authors thank Quat Vu at Intel for many helpful discussions and Bruce Gorris at Caltech for technical assistance. Brad Smith, Dale Hetherington, Jim Fleming, and Tony Farino at Sandia gave valuable input on developing the process flow of the four-point-probe structures. The small-angle diffraction measurement was performed by Greg Beaucage at the University of New Mexico. Financial support for this work was provided by Sandia National Laboratories under Department of Energy Contract DE-AC04-94AL85000 and the Army Research Office.

References

[1] D.K. Schroder, Semiconductor Material and Device Characterization, John Wiley and Sons, New York (1991). Chap. 1.

[2] S.J. Proctor, L.W. Linholm, and J.A. Mazer, *IEEE Trans. Electron Dev.* ED30, 1535 (1983).

[3] S.E. Swirhun, W.M. Loh, R.M. Swanson, and K.C. Saraswat, *IEEE Electron Dev. Lett.*, EDL-6, 639 (1985).

[4] Q.T. Vu, E. Kolawa, L. Halperin, and M-A. Nicolet, *Solid State Electr.* 34, 279 (1991).